

Article

Enhancement of Wood Coating Properties by Adding Silica Sol to UV-Curable Waterborne Acrylics

Yuding Zhu ^{1,†}, Wenkai Zhu ^{1,†} , Zequn Li ¹, Yuan Feng ² , Wei Qi ¹, Song Li ¹, Xiaoyu Wang ^{3,*} and Meiling Chen ^{2,*} 

- ¹ College of Chemistry and Materials Engineering, Zhejiang A&F University, Hangzhou 311300, China
² Jiangsu Co-Innovation Center of Efficient Processing and Utilization of Forest Resources, College of Materials Science and Engineering, Nanjing Forestry University, Nanjing 210037, China
³ Jiangsu Key Laboratory for Biomass-Based Energy and Enzyme Technology, School of Chemistry and Chemical Engineering, Huaiyin Normal University, Huai'an 223300, China
* Correspondence: xwang20@hytc.edu.cn (X.W.); meiling_chen@njfu.edu.cn (M.C.)
† These authors contributed equally to this work.

Abstract: In recent years, with the development of the coating industry and the increasing awareness of environmental protection, the modification of waterborne wood coatings has become the focus of research. Generally, the system composed of silica sol modification and UV curing can make up for the defects of poor mechanical properties, low hardness, and slow curing speeds of waterborne wood coatings. Herein, we used silica sol-reinforced UV-curable waterborne acrylic wood coatings and tested the related physical properties of the coatings. FT-IR analysis showed that the Si-O-Si bond appeared, indicating that the silica sol was successfully grafted onto the waterborne acrylic molecular chain. The results showed that the mechanical properties of the UV-curable waterborne acrylic wood coating film reached their optimum when the content of silica sol was 1 wt%, the number of UV lamps was 3, and the drying time was 20 min. The corresponding values for wear resistance, hardness, adhesion, and impact strength were 0.106 g (high level), grade 3, and 90 kg·cm, respectively. However, when the content of silica sol is greater than 1 wt%, the related physical properties of the coatings will decrease. The results showed that the gloss of the coating decreased with increasing silica sol content. When the silica sol content was 2 wt%–6 wt%, the coating showed a matte gloss. This present work shows that the modification process is simple, controlled, inexpensive, and meets the demand for UV-curable waterborne acrylic wood coatings in daily life.

Keywords: silica sols; waterborne acrylic wood coating; UV-curable; wood paint film performance



Citation: Zhu, Y.; Zhu, W.; Li, Z.; Feng, Y.; Qi, W.; Li, S.; Wang, X.; Chen, M. Enhancement of Wood Coating Properties by Adding Silica Sol to UV-Curable Waterborne Acrylics. *Forests* **2023**, *14*, 335. <https://doi.org/10.3390/f14020335>

Academic Editors: Emilia-Adela Salca, Mohd Hazim Mohamad Amini and Ali Temiz

Received: 28 December 2022
Revised: 1 February 2023
Accepted: 6 February 2023
Published: 8 February 2023



Copyright: © 2023 by the authors. Licensee MDPI, Basel, Switzerland. This article is an open access article distributed under the terms and conditions of the Creative Commons Attribution (CC BY) license (<https://creativecommons.org/licenses/by/4.0/>).

1. Introduction

The coatings used in wood products are collectively referred to as wood coatings, which generally have the effect of protecting the wood and increasing its beauty [1–3]. Wood coatings, as an important coating species, account for up to 10% of the total coatings in each country, thanks to the expansion of the wood industry. Traditional wood coatings contain volatile organic compounds (VOCs) that restrict the utilization and development of traditional wood coatings [4,5]. As a result, the development of low-pollution wood coatings, such as represented by UV-curable water-based wood coatings, has become the focus of scientific research in various countries.

UV-curable water-based wood coatings are a kind of environmental coating that use water as a solvent, can reduce the content of VOCs, and have no irritating odor [6–11]. Moreover, it has many advantages, such as high production efficiency, rapid curing, low energy consumption, low pollution, green environmental protection, and energy savings [12–15]. Due to these advantages, UV-curing waterborne wood coatings are widely used in electronic components, printing, glass, wood coatings, construction, and other industries [16,17]. Therefore, the development of low-pollution wood coatings represented

by UV-curable water-based wood coatings has become the focus of scientific research in various countries. However, because the raw materials of UV-curable waterborne wood coatings mostly come from toluene diisocyanate, which has a low double bond content and a low relative molecular mass, the mechanical properties are poor. The mechanical properties and application range of UV-curable waterborne wood coatings could be improved by certain means. Therefore, it is meaningful and necessary to enhance the relevant performance of UV waterborne wood coatings in this work.

Waterborne acrylic (WA) coating has become one of the main coatings for wood because of its low price, colorlessness, transparency, good light resistance, weather resistance, heat resistance, and construction [18–21]. However, WA coatings also have some disadvantages, such as poor mechanical properties, low hardness, and slow curing speeds, which limit their application to a certain extent. Because of the poor mechanical properties of WA wood coatings, researchers have put forward a variety of solutions. The modification of WA coatings with microcapsules, silane coupling agents, nano-silica, graphene, nano-cellulose, and other materials has achieved certain results [22–26]. Given the slow curing speed of waterborne polyacrylate wood coatings, UV curing can significantly improve the curing efficiency of WA wood coatings [27]. Thus, it is meaningful to modify the UV-curable WA wood coatings to improve their physical properties.

Silica sol is a dispersion system of silica particles in water or a solvent that is odorless, non-toxic, and has a milky white translucent appearance [28,29]. Silica sol is widely used in papermaking, architectural coatings, and electronic industries due to its excellent properties, such as high rigidity, high strength, ultraviolet absorption, high adsorption, high dispersion, and green non-toxicity [30–32]. WA wood coatings' mechanical properties, solid content, UV aging resistance, and thermal insulation, and other properties cannot meet use requirements due to UV curing [33–35]. However, silica-sol colloidal particles have a considerable specific surface area and the particles themselves are colorless and transparent, which does not affect the original color of the covered material. Therefore, silica sol can modify the disadvantages of UV-curable WA coatings. In this study, the use of silica sol to enhance UV-curable WA wood coatings and improve the mechanical properties (wear resistance, hardness, adhesion, and impact resistance) and optical properties of the enhanced coatings is novel and unique.

In this study, we prepared our own silica sol and mixed it in a specific proportion with UV-curable WA coating. Subsequently, the mechanical and optical properties of the UV-curable WA wood coatings reinforced by silica sol were studied. The purpose of this study was to improve the wear resistance, hardness, adhesion, and impact resistance of the coating and to provide a theoretical basis for the industrial application of UV-curing waterborne wood coatings.

2. Materials and Methods

2.1. Materials

Eucalyptus multilayer board (100 × 100 × 5 mm) and UV-curable waterborne acrylic (WA) wood coating were supplied by Guangdong Yihua Wood Industry Co., Ltd. (Shantou, China). Ammonia, anhydrous ethanol, and tetraethyl orthosilicate were purchased from Nanjing Lisheng Chemical Company (Nanjing, China). Distilled water was prepared in the laboratory and used in the entire experiment. Moreover, other reagents were used directly, without any treatment.

2.2. Preparation of Silica Sol

At first, 3 mL of 25 wt% ammonia was poured into a solution containing 50 mL of anhydrous ethanol. Subsequently, the mixture was stirred for 30 min at 25 °C on a magnetic stirrer (RH BASIC S025, Aika Instrument Equipment Co., Ltd., Guangzhou, China). Then, 3 mL of tetraethyl orthosilicate was measured and added drop by drop to the above-mixed solution. After 2 h of magnetic stirring, the silica sol was obtained.

2.3. Preparation of UV-Curable WA Coating Reinforced by Silica Sol

A UV-curable WA coating was reinforced with different contents of silica sol by a mechanical blending method. Briefly, we weighed 3 g of UV-curable WA resin into a beaker and stirred for ten minutes. Then, the silica sol was added to the resin solution at 1 wt%, 2 wt%, 3 wt%, 4 wt%, and 5 wt% of the UV-curable WA resin mass (Table 1). Subsequently, to obtain a uniform dispersion, it was stirred with a magnetic stirrer at 450 r/min for 2 h at 25 °C. Finally, the mixed solution was sonicated with an ultrasonic crusher (HN-150Y, Jinan Tongxin Biotechnology Co., Ltd., Jinan, China) for 10 min to make silica sol uniformly dispersed in the UV-curable WA resin emulsion.

Table 1. The experimental materials and dosage.

Samples	Addition Amount	
	UV-Cured WA Coating (g)	Silica Sol (g)
0	3	0
1	3	0.03
2	3	0.06
3	3	0.09
4	3	0.12
5	3	0.15

2.4. Preparation of the Reinforced Coating

To test the coating film properties of the reinforced coating, it was applied to the surface of the eucalyptus multilayer board with a spray gun (G15/G40, Graco, Philadelphia, PA, USA). Typically, the modified WA is poured into the can of the spray gun. Then, spraying the eucalyptus multilayer board by the “crossed” method, the paint output per gun was controlled at 50 g/cm². At last, the sprayed samples were placed in the drying oven (DZF-6012, Shanghai Yiheng Scientific Instrument Co., Ltd., Shanghai, China) at 40 °C for 3 h. They will be taken out to test the related physical properties. The preparation process for reinforced coating is shown in Figure 1.

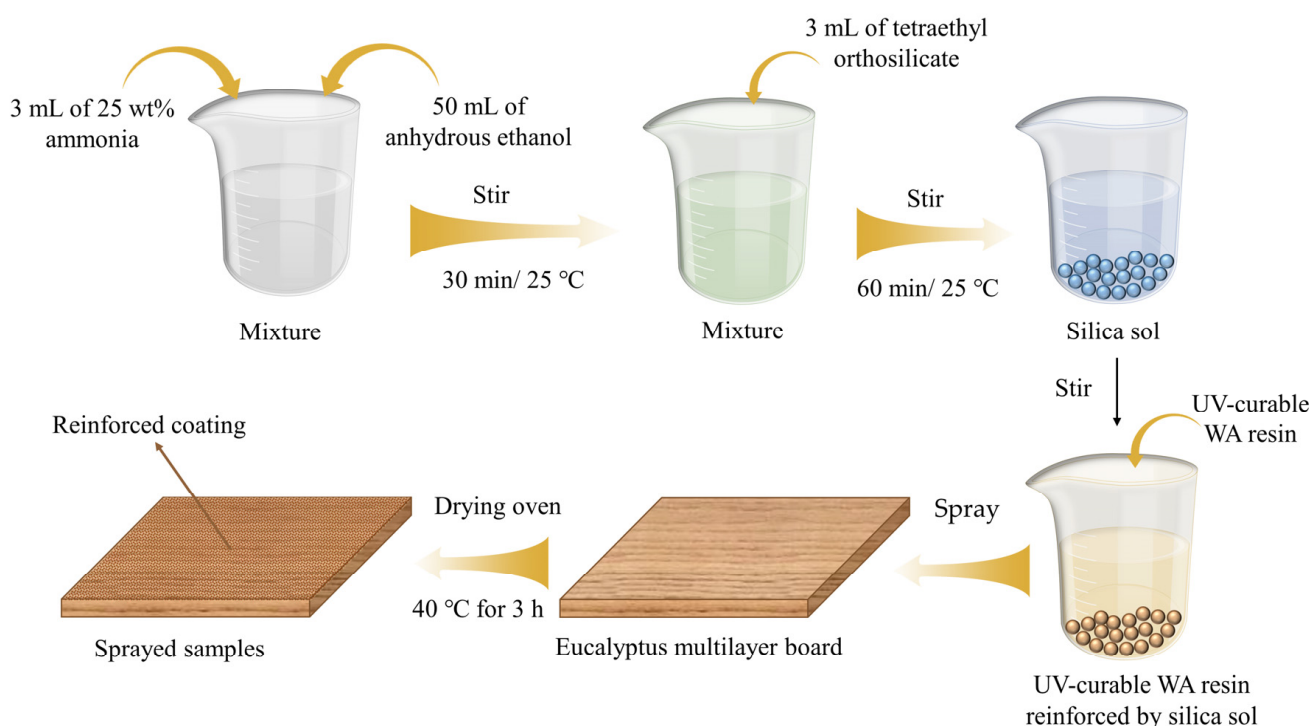


Figure 1. Schematic diagram of the preparation process for the reinforced coating.

2.5. Characterizations

The particle size distribution of silica sol was carried out using a laser particle size analyzer (SALD-2300, Shimadzu Co., Ltd., Kyoto, Japan). A scanning electron microscope (SEM, JEOL-7800F) was carried out to observe the morphology of silica sol and coatings. Fourier transform infrared spectroscopy (FT-IR, Nicolet iS10, Thermo Electron Corp., Madison, WI, USA) was operated to determine the characteristic absorption peaks of UV-curable WA coatings before and after silica sol enhancement. Furthermore, the physical properties of UV-curable WA coating were examined in accordance with the relevant Chinese Standards. The abrasion resistance was carried out using JM-V (Shanghai Tianchen Modern Environment Co., Ltd., Shanghai, China). We calculated the abrasion resistance of the eucalyptus multilayer board after 100 times of grinding, and the unit of abrasion resistance was mg/100 r according to GB/T 18103-2013. The pencil hardness method was adopted to analyze the hardness of the coating (GB/T 23999-2006). The adhesion of the coating was tested by a paint film scribe at 2 mm intervals according to GB/T 7657-2013. Meanwhile, the adhesion level was evaluated according to the peeling of the paint film. The impact resistance test is completed under the guidance of GB/T 7657-2013. The gloss of the UV-curable WA coating was tested by the glossmeter (BGD512-60, KSJ Photoelectrical Instruments Co., Ltd., Quanzhou, China) according to GB/T 9754-2007. Moreover, all the data were analyzed by analysis of variance.

3. Results and Discussion

3.1. Particle Size and SEM Analysis

According to the particle size test results in Table 2, the particle size distribution diagram of the silica sol is shown in Figure 2a. According to the test results in Table 2, when the silica sol concentration was 0.63 mol/L, the average particle size was 34.638 μm . Furthermore, the particle size of silica sol samples less than 62.938 μm accounted for 90% of the total, and 50% were smaller than 29.153 μm . Figure 2a shows the distribution range of the particle size of the silica sol. The particle size distribution of the sample was between 10 and 100 μm . Therefore, the analysis in Figure 2a is consistent with that in Table 2.

Table 2. Particle size test data results.

Items	$D_{10}/\mu\text{m}$	$D_{50}/\mu\text{m}$	$D_{90}/\mu\text{m}$	$D_{av}/\mu\text{m}$	$S:V/(\text{cm}^2 \cdot \text{cm}^{-3})$	$D [3, 2]/\mu\text{m}$	$D [4, 3]/\mu\text{m}$	Fitting Error
Data	11.117	29.153	62.938	34.638	2 677.672	22.408	34.638	0.007

Where D_{av} represents the average particle size of the silica sol, D is the volume average particle size, S/V is the specific surface area, and D_{10} represents 10% of the total volume for particles smaller than 11.117 μm , as are D_{50} and D_{90} . This test adopted the intensity method of the laser particle size analysis to calculate the particle size.

The silica sol and the coatings before and after enhancement were observed under SEM, and the results are shown in Figure 2b–e. As can be seen from Figure 2b,c, the particle size of the as-prepared silica sol was relatively uniform and presented a spherical shape. The SEM images of the silica sol were consistent with the above particle size analysis. It can be seen from Figure 2d that the unmodified UV-curable WA resin coating had cracks and poor thermal stability, which were caused by the contraction of resin molecules when cold. And there was no granular substance in its coating film. However, as shown in Figure 2e, the surface layer of the reinforced film was evenly distributed with some white granular substances. Moreover, these particles were somewhat blurred in the SEM image, and their clear shape cannot be seen. It can be seen that the silica sol particles were not on the surface of the coating film but were coated in the inner layer. Therefore, the addition of silica sol enhanced the stability, hardness, water resistance, and alcohol resistance of the UV-curable WA film.

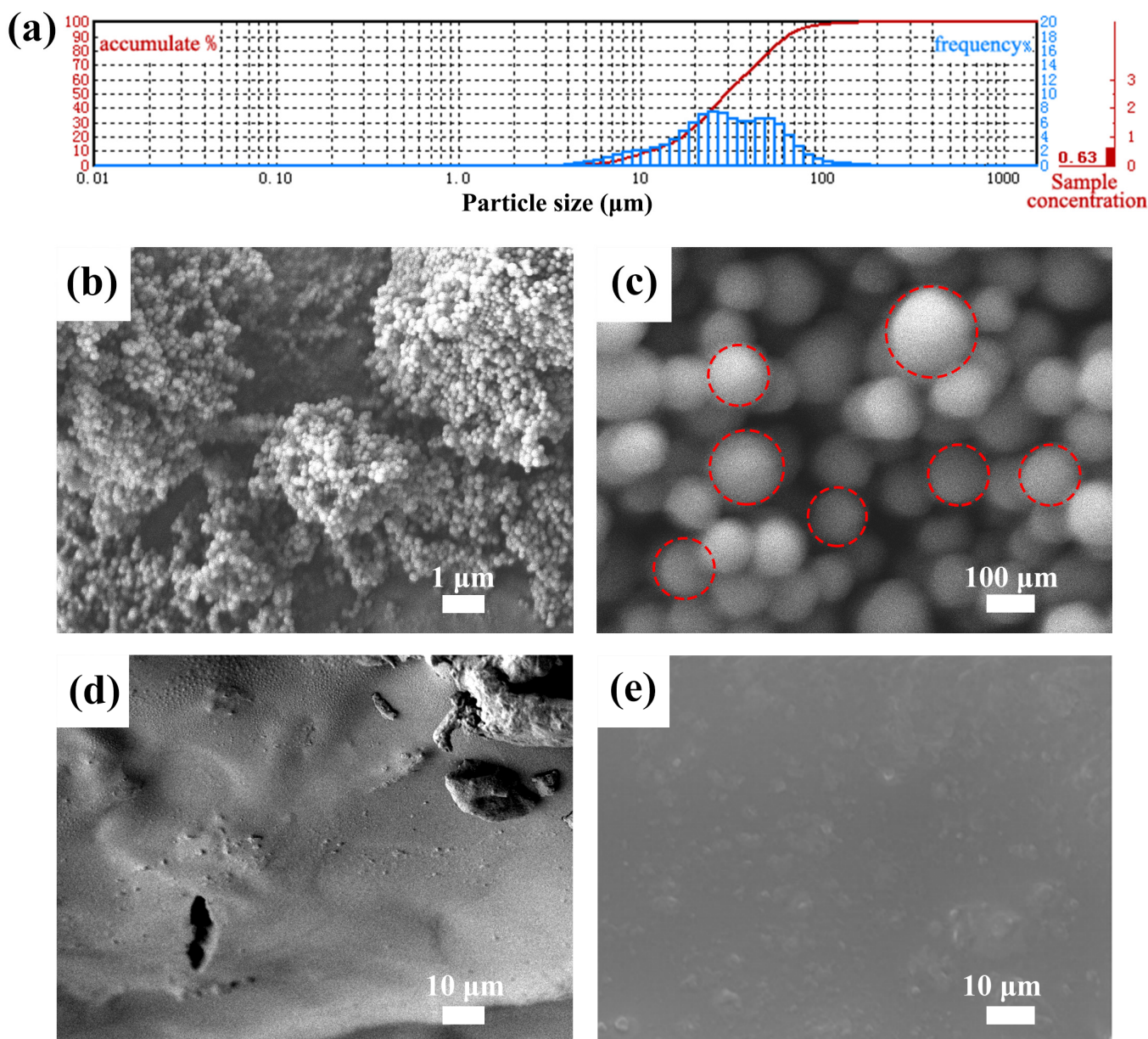


Figure 2. (a) Particle size distribution of silica sol, (b,c) SEM images of silica sol, UV-curable WA coatings before (d) and after (e) being reinforced by silica sol.

3.2. FT-IR of Reinforced Coating

To reveal the characteristic functional group of the reinforced coating, FT-IR spectra were introduced (Figure 3). As shown in Figure 3, these characteristic peaks of the reinforced coating were consistent with the raw materials. Moreover, the solvent of the UV-curable WA resin was water, and the FT-IR analyses were performed by the attenuated total reflection method. The characteristic stretching vibration absorption peak at 3400 cm^{-1} is attributed to -OH. Meanwhile, the characteristic absorption peaks at 2960 cm^{-1} , 2870 cm^{-1} , and 1730 cm^{-1} are methyl, methylene, and carbonyl, respectively. The hydroxyl peaks at 3428 cm^{-1} narrowed with the addition of silica sol, which was due to the reduction of hydroxyl groups as a result of the dehydration condensation reaction between some hydroxyl functional groups on the UV WA resin molecules and the hydroxyl groups on the surface of the silica sol [36]. The FT-IR spectra of the added silica sol showed a significant enhancement of the stretching vibration peak at approximately $1000\text{--}1200\text{ cm}^{-1}$, which was attributed to the condensation of the hydroxyl group on the silica sol with the silicon

hydroxyl group on the main chain to form Si-O-Si [37]. However, the disappearance of the absorption peak of the epoxy group at 910 cm^{-1} is caused by the ring-opening reaction of the epoxy group present in the silica sol with the hydroxyl group on the main chain. The addition of silica sol makes the C=C vibration absorption peak at 829 cm^{-1} weak and narrow, indicating that the double bond between silica sol and the double bond on the main chain of UV WA resin has a cross-linking reaction under UV light. Therefore, the silica sol was successfully grafted onto the UV-WA resin chain by bridging action.

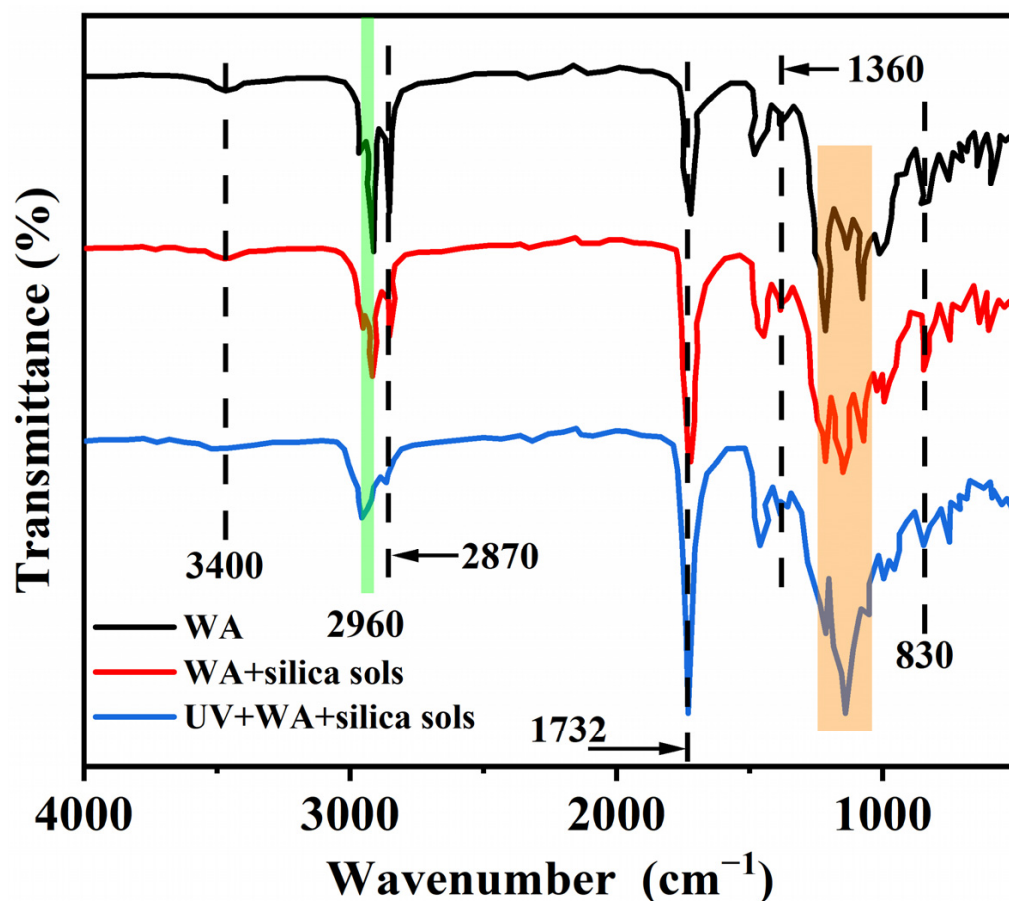
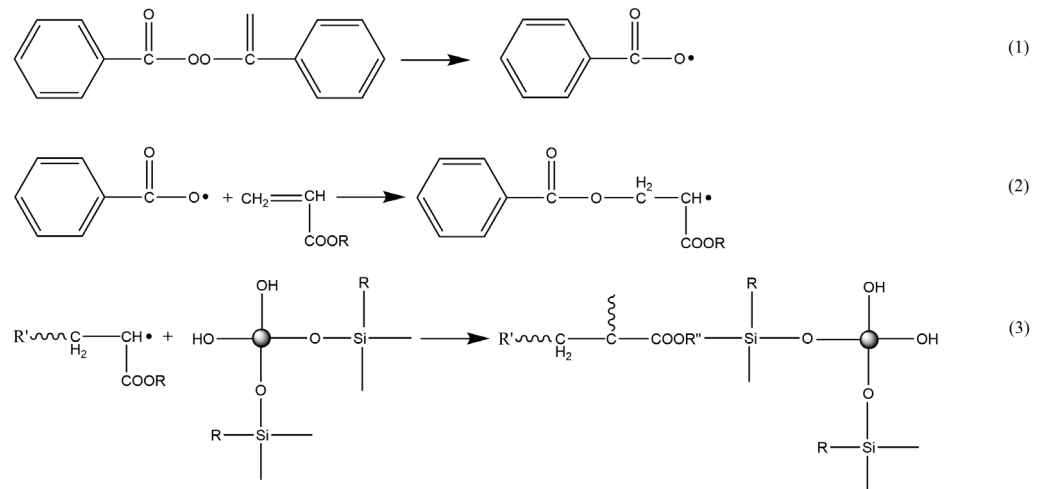


Figure 3. The FT-IR spectra of UV-curable WA before and after being reinforced by silica sol with a 2 wt% concentration.

3.3. Mechanism Analysis

The reaction mechanism of silica sol-reinforced UV-curable WA is shown in the following equations (Equations (1)–(3)). WA and its ester monomers are prepared by solution polymerization, which belongs to free radical polymerization. The addition of silica sol will open the π bond of the WA monomer and undergo an addition reaction to form monomer free radicals (Equations (1) and (2)). Monomer free radicals combine to form molecular chains one at a time. The addition of silica sol increases the number of primary free radicals, which increases the chance of chemical bonding between silica sol and the WA molecule. Therefore, silica sol can be more fully grafted onto the WA molecule. In addition, silica sol can react with active functional groups in WA molecules to form high-energy chemical bonds (Equation (3)). However, when the silica sol was excessive, a large number of active centers will be generated in the system. This will increase the rate of heat generation and chain transfer. The stability of lotion becomes worse, and the precipitation amount increases due to the increase in branch chains generated on the molecule.



3.4. Abrasion Resistance Analysis

Figure 4 shows the influence of the proportion of silica sol in the UV-curable WA coating on the abrasion resistance. And take the average of the three values as the final value of the weight loss. It can be seen from Figure 4 that when the proportion of silica sol in the coating reached 1–3 wt%, the abrasion resistance of the coating was significantly improved. However, when the proportion of silica sol was higher than 3 wt%, the wear resistance of the composite coating decreased. When the content of silica sol is 3 wt%, the lowest wear value is only 0.092 g. When the silica sol content was increased to 4 wt% and 5 wt%, the weight loss was significantly increased to 0.123 g and 0.128 g, respectively. At this time, the weight loss was higher than that of the unmodified coating. Meanwhile, according to the variance analysis, when the silica sol content was 1 wt%, 2 wt%, or 3 wt%, the abrasion resistance of the coating was significantly affected ($p < 0.01$). The reason for this phenomenon is that a small amount of SiO_2 particles in silica sol can significantly improve the coating's wear resistance while having no effect on its transparency. With the increased use of silica sol as an additive, the phenomenon of self-agglomeration occurs due to the uneven distribution of SiO_2 in the coating solution caused by its large specific surface area [38]. As a result, the wear value of the coating increases, which also means that the abrasion resistance of the reinforced coating decreases.

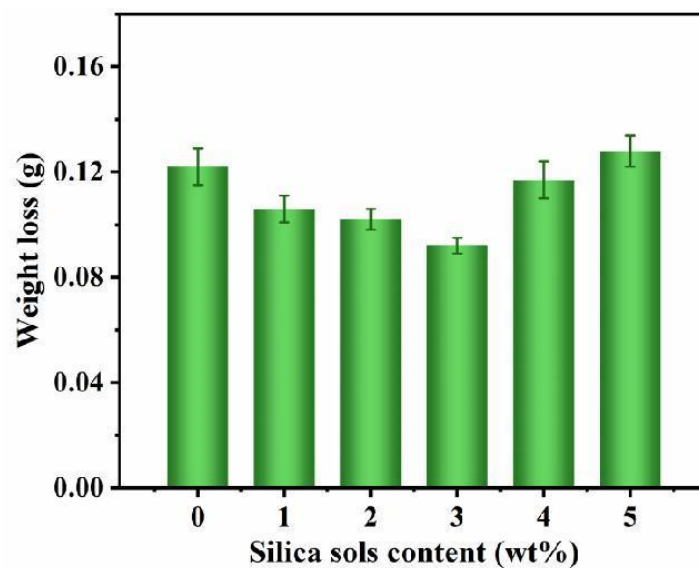


Figure 4. Effect of silica sol content on the abrasion resistance of UV-curable WA coatings.

3.5. Hardness Analysis

The effect of silica sol content on the hardness of UV-curable WA coatings is shown in Figure 5. It can be seen from the figure that when the silica sol content reached 1 wt%, the hardness of the composite coating reached a high level, and the hardness was significantly improved. Although the amount of silica sol was small, it can fully react with UV-curable WA coatings to generate chemical bonds, which can significantly increase the hardness of the paint film [39]. However, the hardness of the coating film decreased when the silica sol content gradually increased. This is due to the uneven dispersion of silica in the silica sol, which makes the coating unable to form a continuous network structure. This is consistent with the results of the abrasion resistance of the composite coating discussed above. However, when the content of silica sol is 5 wt%, excessive SiO₂ will be deposited on the surface of the coating. This will instantly improve the hardness of the coating. Moreover, analysis of variance showed that the coating hardness was not significantly affected by silica sol content ($p > 0.05$). Therefore, when the percentage of silica sol in the coating was 1 wt%, the UV-curable WA coating reinforced by silica sol had excellent abrasion resistance and pencil hardness.

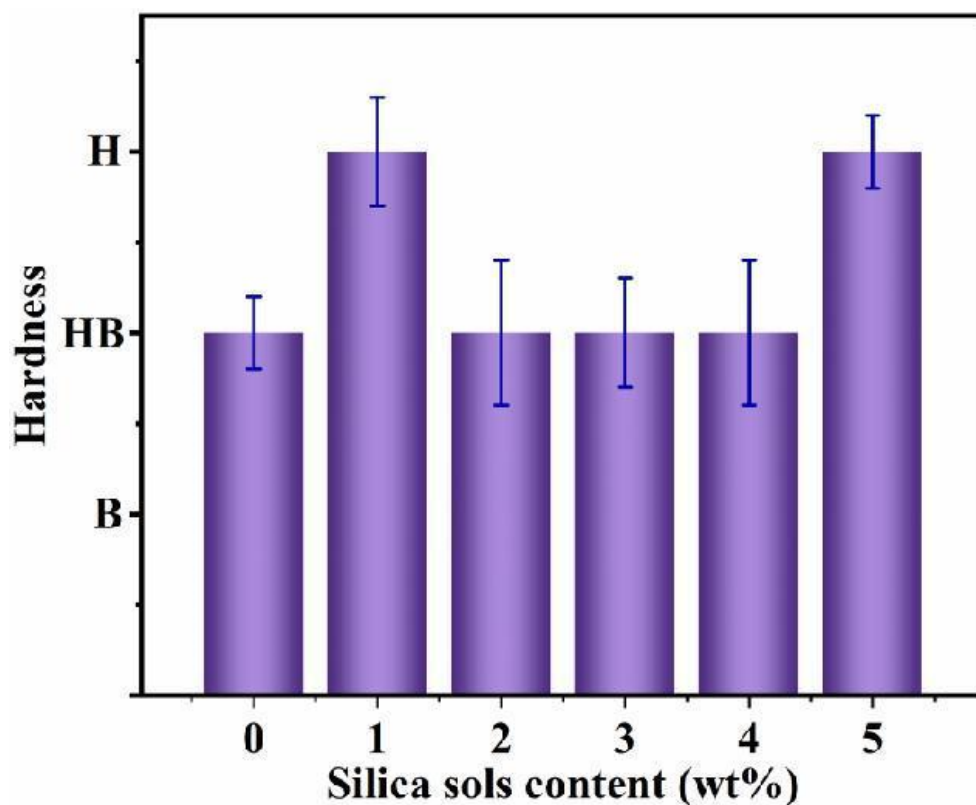


Figure 5. Effect of silica sol content on the hardness of UV-curable WA coatings.

3.6. Adhesion Analysis

Figure 6 shows the effect of silica sol content on the adhesion of the UV-curable WA coating. Generally, the evaluation level of adhesion is from 1 to 7, and level 1 indicates that the adhesion of the coating reached the highest level. It can be seen from Figure 5 that the amount of silica sol additive had a significant effect on the adhesion of the composite coating. Meanwhile, the smaller the amount of added silica sol, the higher the adhesion level was. Furthermore, the adhesion level of the coating becomes smaller and the adhesion decreases as the addition of silica sol increases. When the content of silica sol was 1 wt%, the adhesion of the coating film reached grade 3. When the content of silica sol was 2 wt% to 4 wt%, the adhesion of the coating film remained at level 4. When adding silica sol to 5 wt%, the adhesion continues to decrease to level 5. The analysis of variance showed that

the silica sol content had a significant impact on the adhesion of the coating ($p < 0.01$). The adhesion of the coating refers to the firmness of the bond between the coating film and the substrate, which directly affected the ability of the coating to protect the substrate. When the silica sol was less, it can fully react with UV-curable WA coatings to make the internal and external stress of the coating reached a balance, so that the adhesion of the coating was enhanced. However, when there was too much silica sol, the reaction will be incomplete and a stable structure cannot be formed [40]. The firmness of the combination of the coating film and the substrate was reduced, thereby reducing the adhesion of the coating.

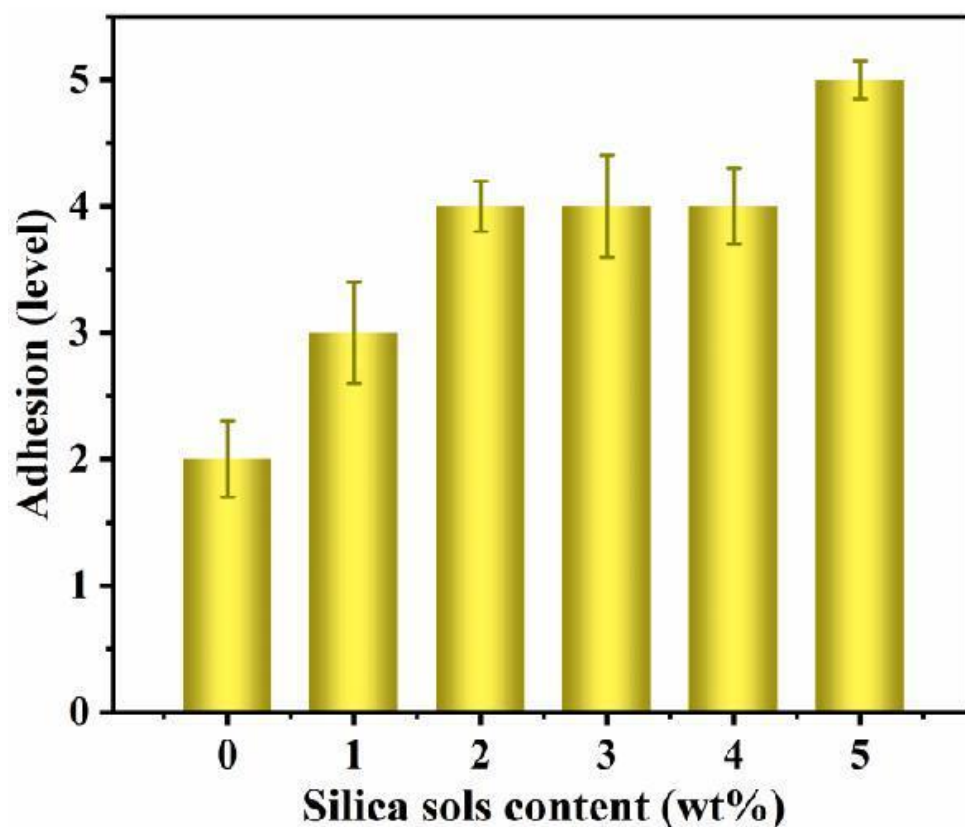


Figure 6. Effect of silica sol content on the adhesion of UV-curable WA coatings.

3.7. Impact Resistance Analysis

The effect of silica sol content on the impact resistance of UV-curable WA coating film is shown in Figure 7. The impact resistance test of the coating surface was used to detect the dynamic loading capacity of the coating surface. Figure 7 shows that when the content of silica sol was 1 wt%, the impact resistance of the coating reached 90 kg·cm, which was significantly better than that of the coating without silica sol. When the silica sol continued to be added, the impact resistance of the coating decreased but was still higher than the 50 kg·cm of the coating without silica sol. An analysis of variance ($p < 0.01$) showed that the impact resistance of the coating was significantly affected when the silica sol content was between 1 wt% and 2 wt%. However, the factor analysis showed that when the silica sol content was 3 wt%, 4 wt%, or 5 wt%, the p -value was greater than 0.05, indicating that the impact strength had no significant impact. The reason for this phenomenon was that a smaller amount of silica sol can react fully with the UV-curable WA coating substrate to form a chemical bonding interaction, resulting in a significant increase in the impact resistance of the coating layer. As the silica sol content increased, the impact resistance of the coating decreased due to the agglomeration and self-cross-linking reactions of silica particles in the silica sol. Compared with the related literature, this result shows excellent impact resistance performance [2,5].

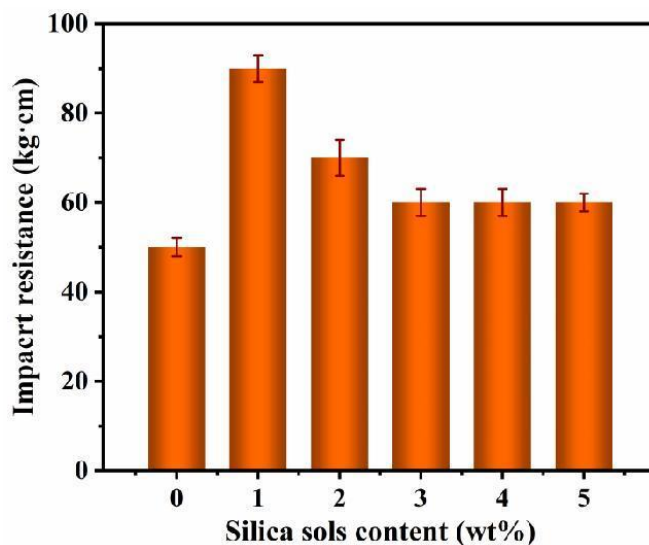


Figure 7. Effect of silica sol content on the impact resistance of UV-curable WA coatings.

3.8. Glossiness Analysis

The glossiness of the UV-curable WA coating modified by silica sol is shown in Figure 8. Moreover, each sample was measured three times, and the average was taken as the final value. As shown in Figure 8, the addition of silica sol had a large impact on the glossiness of the coating. Furthermore, the one-way analysis of variance shows that the content of silica sol has a significant effect on the gloss of the coating ($p < 0.01$). It can be seen from the analysis of two adjacent factors that the p value between them is less than 0.05. Combined with Figure 8, it can be seen that the coating has excellent gloss when the silica sol content is greater than 1 wt%. The gloss of the coating shows a decreasing trend with the increase in silica sol. This is because silica sol is a colloidal solution with fine particles. The high nanoactivity of SiO_2 during gel separation will bind the powder particles in the coating. In addition, SiO_2 forms a new silicate inorganic polymer compound with inorganic salts and metal oxides and further hardens to form a film. Meanwhile, the fine particles are deeply penetrating the substrate and can penetrate its interior via capillary action [41]. Therefore, silica sols reacted chemically with UV-cured WA coatings to produce inorganic opaque substances, which greatly reduced the gloss and transparency of the coating. Accompanied by excellent gloss performance, it also has a certain degree of competitiveness.

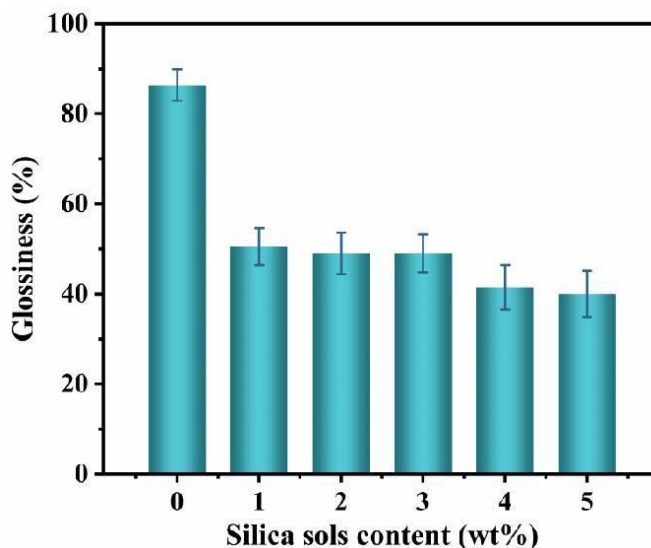


Figure 8. Effect of silica sol content on the glossiness of UV-curable WA coatings.

4. Conclusions

In this study, we investigated the effect of silica sol on the chemical and physical properties of UV-cured WA wood coating films. UV-curable WA wood coatings with superior overall performance were prepared, which improved the mechanical properties of the coatings such as abrasion resistance, hardness, and impact resistance. The results show that when the content of silica sol in the UV-curable WA coating was 1 wt%, the mechanical properties (except adhesion) of the coating could meet the application requirements. At this time, the corresponding weight loss value of the coating was 0.106 g; the hardness had reached grade H, the adhesion had reached grade 3, and the impact resistance had reached 90 kg·cm. The reason for this phenomenon is that silica sol has excellent properties such as high rigidity, high strength, ultraviolet absorption, high adsorption, and high dispersion. Furthermore, the amount of silica sol additive has a great influence on the optical properties of UV-cured WA wood coatings. With the increase in silica sol addition, the optical properties of the coating tend to be matte, which meets the demand of the development of wood coating in the direction of matte. However, the physical/chemical interactions of silica microparticles with WA emulsion and statistical analysis need to be further investigated. This work demonstrates the potential application of silica sol in UV-curable WA wood coatings. Meanwhile, it also provides a new perspective for the design of new UV-cured wood coatings.

Author Contributions: Conceptualization, S.L., X.W. and W.Z.; methodology, Y.Z., Z.L. and M.C.; software, M.C. and S.L.; validation, Y.Z., M.C., W.Q. and W.Z.; formal analysis, Y.F., Y.Z. and W.Q.; investigation, Z.L.; resources, M.C.; data curation, S.L. and X.W.; writing—original draft preparation, Y.F., Y.Z. and M.C.; writing—review and editing, S.L., X.W. and W.Z.; visualization, M.C.; supervision, S.L. and X.W.; project administration, Y.F. and M.C.; funding acquisition, S.L. All authors have read and agreed to the published version of the manuscript.

Funding: This research was funded by the Nanjing Science and Technology Innovation Project for Overseas Students, the Research and Development Funding of Zhejiang A&F University (2022LFR076), the Project Funded by the Natural Science Foundation of Jiangsu Province of China (BK20201072), the National Natural Science Foundation of China (22078123, 32071687), and the Natural Science Foundation of the Higher Education Institutions of Jiangsu Province (19KJB22006).

Institutional Review Board Statement: Not applicable.

Informed Consent Statement: Not applicable.

Data Availability Statement: The data that support the findings of this study are available from the corresponding author, S.L., upon reasonable request.

Acknowledgments: We would like to thank other members in our groups for helping us prepare for the samples. The advanced analysis and testing center of Zhejiang A&F University is acknowledged.

Conflicts of Interest: The authors declare no conflict of interest.

References

1. Rowell, R.; Bongers, F. Role of Moisture in the Failure of Coatings on Wood. *Coatings* **2017**, *7*, 219. [[CrossRef](#)]
2. Wu, L.; Chen, M.; Xu, J.; Fang, F.; Li, S.; Zhu, W. Nano-SiO₂-Modified Waterborne Acrylic Acid Resin Coating for Wood Wallboard. *Coatings* **2022**, *12*, 1453. [[CrossRef](#)]
3. Liu, L.; Shan, H.; Jia, X.K.; Duan, S.J.; Gao, Y.J.; Xu, C.Y.; Wei, S.Y. Study on UV curable tung oil based waterborne polyurethane wood coatings. *J. For. Eng.* **2022**, *7*, 115–121.
4. Wang, J.; Wu, X.; Wang, Y.; Zhao, W.; Zhao, Y.; Zhou, M.; Wu, Y.; Ji, G. Green, Sustainable Architectural Bamboo with High Light Transmission and Excellent Electromagnetic Shielding as a Candidate for Energy-Saving Buildings. *Nano-Micro Lett.* **2023**, *15*, 11. [[CrossRef](#)]
5. Jia, Z.; Bao, W.; Tao, C.; Song, W. Reversibly photochromic wood constructed by depositing microencapsulated/polydimethylsiloxane composite coating. *J. For. Res.* **2022**, *33*, 1409–1418. [[CrossRef](#)]
6. Wu, L.; Zhu, W.; Li, Z.; Li, H.; Xu, J.; Li, S.; Chen, M. Urushiol modified epoxy acrylate as UV spray painting oriental lacquer ink. *RSC Adv.* **2023**, *13*, 1106–1114. [[CrossRef](#)]
7. Dai, Y.; Qiu, F.; Xu, J.; Yu, Z.; Yang, P.; Xu, B.; Jiang, Y.; Yang, D. Preparation and properties of UV-curable waterborne graphene oxide/polyurethane-acrylate composites. *Plast. Rubber Compos.* **2014**, *43*, 54–62. [[CrossRef](#)]

8. Cai, Z.Y.; Zhu, H.X.; Wang, P.; Wu, C.Y.; Gao, W.C.; Mu, J.Y.; Wei, S.Y. Performance optimization of UV curable waterborne polyurethane acrylate wood coatings modified by castor oil. *J. For. Eng.* **2020**, *5*, 89–95.
9. Herrera, R.; Muszyńska, M.; Krystofiak, T.; Labidi, J. Comparative evaluation of different thermally modified wood samples finishing with UV-curable and waterborne coatings. *Appl. Surf. Sci.* **2015**, *357*, 1444–1453. [[CrossRef](#)]
10. Liao, H.; Zhang, B.; Huang, L.; Ma, D.; Jiao, Z.; Xie, Y.; Tan, S.; Cai, X. The utilization of carbon nitride to reinforce the mechanical and thermal properties of UV-curable waterborne polyurethane acrylate coatings. *Prog. Org. Coat.* **2015**, *89*, 35–41. [[CrossRef](#)]
11. Dai, Y.; Qiu, F.; Wang, L.; Zhao, J.; Yu, Z.; Yang, P.; Yang, D.; Kong, L. UV-curable electromagnetic shielding composite films produced through waterborne polyurethane-acrylate bonded graphene oxide: Preparation and effect of different diluents on the properties. *E-Polymers* **2014**, *14*, 427–440. [[CrossRef](#)]
12. Xu, J.; Qiu, F.; Rong, X.; Dai, Y.; Yang, D. Preparation and Surface Pigment Protection Application of Stone Substrate on UV-Curable Waterborne Polyurethane-acrylate Coating. *J. Polym. Mater.* **2014**, *31*, 287–303.
13. Hwang, H.-D.; Moon, J.-I.; Choi, J.-H.; Kim, H.-J.; Do Kim, S.; Park, J.C. Effect of water drying conditions on the surface property and morphology of waterborne UV-curable coatings for engineered flooring. *J. Ind. Eng. Chem.* **2009**, *15*, 381–387. [[CrossRef](#)]
14. Huang, Y.; Ma, T.; Li, L.; Wang, Q.; Guo, C. Facile synthesis and construction of renewable, waterborne and flame-retardant UV-curable coatings in wood surface. *Prog. Org. Coat.* **2022**, *172*, 107104. [[CrossRef](#)]
15. He, Y.R.; Wu, Y.Z.; Zhang, J.P.; Qu, W. Preparation of UV-curing flame-retardant coating for parquet using open paint process. *J. For. Eng.* **2022**, *7*, 174–180.
16. Dai, J.; Ma, S.; Wu, Y.; Zhu, J.; Liu, X. High bio-based content waterborne UV-curable coatings with excellent adhesion and flexibility. *Prog. Org. Coat.* **2015**, *87*, 197–203. [[CrossRef](#)]
17. Song, S.C.; Kim, S.J.; Park, K.-K.; Oh, J.-G.; Bae, S.-G.; Noh, G.H.; Lee, W.-K. Synthesis and properties of waterborne UV-curable polyurethane acrylates using functional isocyanate. *Mol. Cryst. Liq. Cryst.* **2017**, *659*, 40–45. [[CrossRef](#)]
18. Yan, X.X.; Tao, Y.; Qian, X.Y. Preparation of microcapsules for core materials and their effects on properties of waterborne coatings on basswood. *J. For. Eng.* **2022**, *7*, 186–192.
19. Bhavsar, R.A.; Nehete, K.M. Rheological approach to select most suitable associative thickener for water-based polymer dispersions and paints. *J. Coat. Technol. Res.* **2019**, *16*, 1089–1098. [[CrossRef](#)]
20. Yan, X.; Peng, W.; Qian, X. Effect of water-based acrylic acid microcapsules on the properties of paint film for furniture surface. *Appl. Sci.* **2021**, *11*, 7586. [[CrossRef](#)]
21. Kong, X.; Meng, X. Application of Chemical Technology of Water-Based Acrylic Dipping Paint in Art Painting Creation. *J. Chem.* **2022**, *2022*, 7715011. [[CrossRef](#)]
22. Zhu, W.; Ji, M.; Chen, F.; Wang, Z.; Chen, W.; Xue, Y.; Zhang, Y. Formaldehyde-free resin impregnated paper reinforced with cellulose nanocrystal (CNC): Formulation and property analysis. *J. Appl. Polym. Sci.* **2020**, *137*, 48931. [[CrossRef](#)]
23. Kai-li, L.; Qi-ming, F.; Yan-hui, H.; Fan, L.; Quan-fei, H.; Wei, Z.; Xue-cong, W. Effect of Modified Acrylic Water-Based Paint on the Properties of Paint Film. *Spectrosc. Spectr. Anal.* **2020**, *40*, 2133–2137.
24. Goodarzi, I.M.; Farzam, M.; Shishesaz, M.R.; Zaarei, D. Eco-friendly, acrylic resin-modified potassium silicate as water-based vehicle for anticorrosive zinc-rich primers. *J. Appl. Polym. Sci.* **2014**, *131*, 40370. [[CrossRef](#)]
25. Zhang, J.; Bao, Y.; Guo, M.; Peng, Z. Preparation and properties of nano SiO₂ modified cellulose acetate aqueous polymer emulsion for leather finishing. *Cellulose* **2021**, *28*, 7213–7225. [[CrossRef](#)]
26. Fufa, S.M.; Jelle, B.P.; Hovde, P.J. Weathering performance of spruce coated with water based acrylic paint modified with TiO₂ and clay nanoparticles. *Prog. Org. Coat.* **2013**, *76*, 1543–1548. [[CrossRef](#)]
27. Deflorian, F.; Fedel, M.; DiGianni, A.; Bongiovanni, R.; Turri, S. Corrosion protection properties of new UV curable waterborne urethane acrylic coatings. *Corros. Eng. Sci. Technol.* **2008**, *43*, 81–86. [[CrossRef](#)]
28. Yin, Y.; Wang, C.; Wang, Y. Preparation and colloidal dispersion behaviors of silica sol doped with organic pigment. *J. Sol-Gel Sci. Technol.* **2012**, *62*, 266–272. [[CrossRef](#)]
29. Dong, D.; Xiaobo, L.; Wencheng, H. Stability of the Silica Sols Prepared by Acid/Base Two-Step Catalytic Sol-Gel Process. *Rare Met. Mater. Eng.* **2010**, *39*, 61–64.
30. Trupp, L.; Marchi, M.C.; Barja, B.C. Lanthanide-based luminescent hybrid silica materials prepared by sol-gel methodologies: A review. *J. Sol-Gel Sci. Technol.* **2021**, *102*, 63–85. [[CrossRef](#)]
31. Morosanova, E.I. Silica and silica-titania sol-gel materials: Synthesis and analytical application. *Talanta* **2012**, *102*, 114–122. [[CrossRef](#)]
32. Gonçalves, M.C. Sol-gel silica nanoparticles in medicine: A natural choice. Design, synthesis and products. *Molecules* **2018**, *23*, 2021. [[CrossRef](#)]
33. Cristea, M.V.; Riedl, B.; Blanchet, P. Effect of addition of nanosized UV absorbers on the physico-mechanical and thermal properties of an exterior waterborne stain for wood. *Prog. Org. Coat.* **2011**, *72*, 755–762. [[CrossRef](#)]
34. Sangermano, M.; Foix, D.; Kortaberria, G.; Messori, M. Multifunctional antistatic and scratch resistant UV-cured acrylic coatings. *Prog. Org. Coat.* **2013**, *76*, 1191–1196. [[CrossRef](#)]
35. Bongiovanni, R.; Montefusco, F.; Priola, A.; Macchioni, N.; Lazzeri, S.; Sozzi, L.; Ameduri, B. High performance UV-cured coatings for wood protection. *Prog. Org. Coat.* **2002**, *45*, 359–363. [[CrossRef](#)]
36. Al-Thobity, A.M.; Gad, M.M. Effect of silicon dioxide nanoparticles on the flexural strength of heat-polymerized acrylic denture base material: A systematic review and meta-analysis. *Saudi Dent. J.* **2021**, *33*, 775–783. [[CrossRef](#)]

37. Malakauskaite-Petruleviciene, M.; Stankeviciute, Z.; Niaura, G.; Garskaite, E.; Beganskiene, A.; Kareiva, A. Characterization of sol-gel processing of calcium phosphate thin films on silicon substrate by FTIR spectroscopy. *Vib. Spectrosc.* **2016**, *85*, 16–21. [[CrossRef](#)]
38. Zhu, W.; Kim, D.; Han, M.; Jang, J.; Choi, H.; Kwon, G.; Jeon, Y.; Ryu, D.Y.; Lim, S.-H.; You, J.; et al. Fibrous Cellulose Nanoarchitectonics on N-doped Carbon-based Metal-Free Catalytic Nanofilter for Highly Efficient Advanced Oxidation Process. *Chem. Eng* **2023**, 141593. [[CrossRef](#)]
39. Chen, G.; Zhou, S.; Gu, G.; Wu, L. Acrylic-Based Polyurethane/Silica Hybrids Prepared by Acid-Catalyzed Sol–Gel Process: Structure and Mechanical Properties. *Macromol. Chem. Phys.* **2005**, *206*, 885–892. [[CrossRef](#)]
40. Zheng, C.X.; Zhu, S.L.; Lu, Y.; Mei, C.T.; Xu, X.W.; Yue, Y.Y.; Han, J.Q. Synthesis and characterization of cellulose nanofibers/polyacrylic acid-polyacrylamide double network electroconductive hydrogel. *J. For. Eng.* **2020**, *5*, 93–100.
41. Nazarabady, M.M.; Farzi, G.A. Tunable morphology for silica/poly (acrylic acid) hybrid nanoparticles via facile one-pot synthesis. *Macromol. Res.* **2016**, *24*, 716–724. [[CrossRef](#)]

Disclaimer/Publisher’s Note: The statements, opinions and data contained in all publications are solely those of the individual author(s) and contributor(s) and not of MDPI and/or the editor(s). MDPI and/or the editor(s) disclaim responsibility for any injury to people or property resulting from any ideas, methods, instructions or products referred to in the content.